

## PROTOTYPE AND MODEL OF SOLAR DRIVEN DESALINATION PLANT IN ARID ENVIRONMENT

by

***Koichi UNAMI<sup>a\*</sup>, Osama MOHAWESH<sup>b</sup>, and Masayuki FUJIHARA<sup>a</sup>***

<sup>a</sup>Graduate School of Agriculture, Kyoto University, Kyoto, Japan

<sup>b</sup>Deanship of Scientific Research, Mutah University, Karak, Jordan

Original scientific paper

<https://doi.org/10.2298/TSCI180604097U>

*Water shortage and salinity are crucial factors affecting plant growth in arid and semi-arid regions, where irrigation water shortage and capillary rise from shallow saline water tables are often encountered. The objectives of this study are to construct a prototype of solar driven desalination plant in an arid area of Jordan Rift Valley, to develop a mathematical model predicting thermal dynamics in the prototype, to calibrate model parameters with measured physical parameters, and to discuss the performance of the prototype as well as its applicability to other areas under different environment. Results of measurement and numerical simulation show that the model is capable to reproduce the thermal dynamics of the desalination plant and to predict dew yield. Overall, the developed model provides a sound basis for describing and explaining the mass and energy balance mechanisms in the developed desalination plant. This study offers also a useful tool for analysis and assessment of the dew yield and thermal dynamics of such a desalination plant in general. Using the constructed prototype, performance analysis based on crop cultivation is ongoing.*

Key words: *water scarcity, solar desalination, dew collection, thermal dynamics, arid environment*

### Introduction

Water shortage and salinity are crucial factors affecting plant growth in arid and semi-arid regions, where irrigation water shortage and capillary rise from shallow saline water tables are often encountered, Salamah [1]. An increasing demand for water, particularly in arid and semi-arid regions, has enforced farmers to use low-quality water sources such as brackish water, saline ground-water, and leaching return-flow water for irrigation, Mohawesh [2]. The level of salinity of such water imposed the importance to treat and desalinate this water to retain sustainable agricultural practices. In light of the addressed water-related problems, sustainable methods to tackle water shortage are essential, Unami *et al.* [3].

The scarcity and erratic nature of rainfall make this option a viable solution, Unami and Mohawesh [4]. This can be achieved using a technology called humidification-dehumidification greenhouses (GH), Perret *et al.* [5] and Jolliet [6]. Water desalination driven by solar energy can help to solve the main problems associated with irrigation water demand, mainly for protected cropping. Desalination process needs considerable quantities of energy to attain separate of salt from saline water. The economic and environmental costs of conventional ener-

\* Corresponding author; email: [unami@adm.kais.kyoto-u.ac.jp](mailto:unami@adm.kais.kyoto-u.ac.jp)

gy sources for water desalination highlighted the solar energy, as a potential power source for desalination. Renewable energy systems, which utilizing freely available energy source (solar energy) are sensible sustainable solutions.

Desalination looks appropriate where saline or brackish water is available. The cost of power desalination is not practical methods for arid land farming, Goosen *et al.* [7]. Several countries are facing water shortage, however, they most benefit from solar energy potential. This desalination method can offer a viable key to supply arid lands with fresh water, Chaibi [8]. The approach is to use solar energy through evaporation, to humidify and saturate the air inside the GH dew collection system including a saline water reservoir. If its temperature is falling below the dewpoint, which usually happened during the night, condensation of fresh water should potentially occur, Hao *et al.* [9]. This system can be incorporated into the design of the GH in arid regions. Greenlee *et al.* [10] stated that desalination is a valuable means of securing water for drinking and agricultural irrigation. Desalination offers a novel and extra water resource for irrigated agriculture. Malik *et al.* [11] experimentally examined the potential use of GH fitted with solar desalination systems for small-scale farming in areas where only saline or brackish water is available. Several studies of solar desalination and its application GH irrigation have been conducted. Chaibi [12] used simulation model and experiments to explore a GH roof integrated desalination system. He found that the system could be used as a means of supplying irrigation water to GH crops in an arid environment. Medina [13] indicated that the use of water desalination in agriculture is practical. Zhani [14] found that a suitable distilled water quality for irrigation was obtained using a theoretical and experimental solar desalination study. Mashaly *et al.* [15] found that 1 m<sup>2</sup> of solar-still systems was found to meet the crop water requirement (CWR) of about 2 m<sup>2</sup> of protected cultivation in Saudi Arabia.

A considerable part of the Middle East and North Africa (MENA) region are in such a harsh environment with a precipitation of less than 100 mm per year, Oroud [16] and Matouq [17]. Mohawesh [2] stated that an agricultural irrigation made up approximately 70% of Jordan's water consumption, where agriculture is the primary job activity and a key role in food security. The Jordan Rift Valley is several degrees warmer than adjacent areas and is compared to function as a giant GH, due to the unique location and all-year good climate conditions, Mohawesh [18]. The agriculture in Jordan Rift Valley is totally depending on water for irrigation, Molle *et al.* [19]. However, increased water scarcity, low rainfall and its uneven distribution, high losses due to evaporation and surface runoff, increased demand due to population growth and deteriorating water qualities are major problems affecting agricultural productivity.

In Jordan Rift Valley, farming is commonly practiced using plastic mulches and trickle irrigation systems. This practice is suitable and effective in Jordan Rift Valley, both in open fields or under GH due to its advantages in preserving the limited irrigation water resources, Amayreh and Al-Abed [20] and Mahadeen *et al.* [21]. The aim of the protected cultivation is not only to provide a suitable environment for crop growth but also it decreases CWR. The average daily open field CWR in the southern part of the Jordan Rift Valley under mulched and drip irrigation system is 3 mm per day, [22]. However, protected cultivation requires less water than open-field agriculture, with a reduction in CWR of approximately 20-50%, Harmanto *et al.* [23]. The southern part of the Jordan Rift Valley is characterized by the lowest precipitation due to its elevation below mean sea level (-420 m below sea level) and by the high salinity along the coast of the Dead Sea. In Lisan Peninsula (LP) near the south end of the Dead Sea, the aridity coupled with over-pumping of ground-water has often resulted in water quality deterioration. Irrigating with low water quality has resulted in increasing soil salinity. Accordingly, many cultivated lands in LP are being abandoned or less productive, Ammari *et al.* [24]. This requires

securing freshwater for irrigation, which can be achieved by instigating suitable methods for exploiting of saline/brackish water sources.

Therefore, the objectives of this study are construct a prototype of solar driven desalination plant in LP, to develop a mathematical model predicting thermal dynamics in the prototype, to calibrate model parameters with measured physical parameters, and to discuss the performance of the prototype as well as its applicability to other areas under different environment.

## Methodology

### Construction of prototype

The prototype of solar driven desalination plant has been established at Agricultural Research Station of Mutah University ( $31^{\circ} 15' 33''$  N,  $35^{\circ} 29' 22''$  E), located in LP of Jordan Rift Valley, Jordan. The only source of water at the site is a flash flood harvesting system. An intake structure constructed at the downstream end of a valley having a  $1.12 \text{ km}^2$  barren watershed diverts ephemeral flash floods occurring in the valley into an open-air reservoir, Sharifi *et al.* [25]. Despite being surface runoff, the harvested water is relatively saline due to high salinity of the watershed. This has motivated construction of such a desalination plant. As shown in fig. 1, the prototype is indeed an innovated GH with 9 m width, 51.00 m length, 4 m height under the ridge, and 2.05 m height at the roof eaves (gutter), making a global volume of  $1644 \text{ m}^3$  and a cross-section area of  $32.23 \text{ m}^2$ . The long axis is oriented in NNW-SSE direction. The structure of GH is of metal frames covered with polyethylene (PE) sheets with a thickness of 0.18 mm and a specific gravity of  $1400 \text{ kg/m}^3$ . The floor of GH has been dug out to 1.3-1.8 m deep to create another reservoir (GH reservoir) with a surface area of  $220 \text{ m}^2$  and then fully covered with polyvinyl chloride (PVC) sheets with a thickness of 0.03 mm and a specific gravity of  $1320 \text{ kg/m}^3$ . Dew condensation occurring along the GH cover functions as desalination of the saline water, which is transferred from the open-air reservoir to the GH reservoir by pump. Water repellent cloth (WRC) with a thickness of 0.10 mm and a specific gravity of  $1350 \text{ kg/m}^3$  has been utilized for efficient collection of the dew: adsorbed dew on the GH cover turns into drips, which either fall or follow the GH cover down to the WRC set along GH sides. Thin plastic sheets are attached to GH eaves to connect the GH sides with WRC. Each piece of WRC (3.00 m long and 1.47 m width) was holed at five points (center point and four corners); a grommet was fixed to each point. The central grommet represents a discharge point. Each WRC was tied to GH latitudinal bars using grommet holes at the corners with a 3 m interval at a height of 2.05 m. A small gravel bag weighting around 0.2-0.3 kg coupled with a PET bottle was hanged from the center grommet on each piece of WRC, to direct collected dew into the WRC discharge point (center grommet) and then to the PET bottle. There are 29 pieces of WRC (14 pieces on the right side, and 15 pieces on the left side), and the total area of WRC is  $135 \text{ m}^2$ .

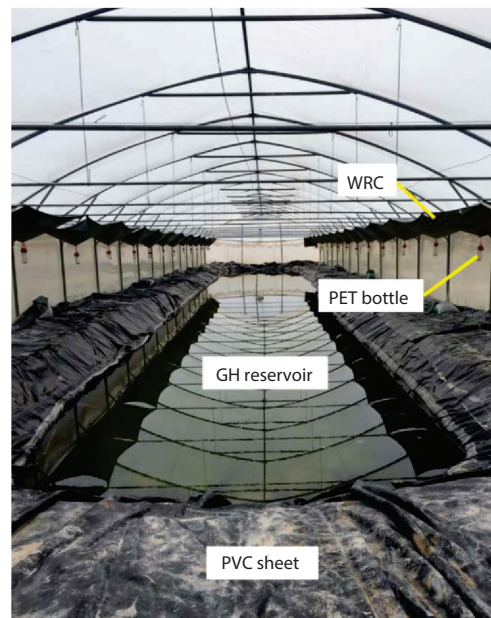


Figure 1. Inside view of the innovated GH functioning as a desalination plant

*Mathematical modeling*

The desalination plant is modeled as an aggregation of six media: ambient ( $M_0$ ), GH reservoir ( $M_1$ ), GH ground ( $M_2$ ), GH air ( $M_3$ ), WRC ( $M_4$ ), and GH cover ( $M_5$ ). In order to represent the dynamics of the interacting six media, three water mass balance equations and five energy balance equations are considered:

$$\begin{aligned}\frac{dV_1}{dt} &= Q_{01} - Q_{12} - Q_{13} - Q_{15} \\ \frac{dV_3}{dt} &= Q_{13} - Q_{35} \\ \frac{dV_5}{dt} &= Q_{15} + Q_{35} + Q_{45}\end{aligned}\quad (1)$$

and

$$\begin{aligned}\frac{d}{dt}(C_1 m_1 T_1) &= P_{01} - P_{12} - P_{13} - P_{14} - P_{15} \\ \frac{d}{dt}(C_2 m_2 T_2) &= P_{02} + P_{12} - P_{23} - P_{24} - P_{25} \\ \frac{d}{dt}(C_3 m_3 T_3) &= P_{03} + P_{13} + P_{23} - P_{34} - P_{35} \\ \frac{d}{dt}(C_4 m_4 T_4) &= P_{04} + P_{14} + P_{24} + P_{34} - P_{45} \\ \frac{d}{dt}(C_5 m_5 T_5) &= P_{05} + P_{15} + P_{25} + P_{35} + P_{45}\end{aligned}\quad (2)$$

where  $t$  is the time,  $V_i$  – the volume of water stored in the medium  $M_i$ ,  $Q_{ij}$  – the water mass flux flowing from the medium  $M_i$  to the medium  $M_j$ ,  $T_i$  – the temperature of the medium  $M_i$ ,  $C_i$  – the heat capacity of the medium  $M_i$ ,  $m_i$  – the mass of the medium  $M_i$ , and  $P_{ij}$  – the heat flux flowing from the medium  $M_i$  to the medium  $M_j$ . According to Sun *et al.* [26], the heat capacity  $C_1$  of the saline water  $M_1$  in GH reservoir is approximately given:

$$C_1 = C_{\text{wat}} - 4.4c \quad (3)$$

where  $C_{\text{wat}}$  is the heat capacity of freshwater, and  $c$  – the concentration of salt. As the medium  $M_3$  is a mixed gas, the heat capacity  $C_3$  depends on  $m_3$ , and  $T_3$ :

$$C_3 = C_{\text{dry}} + (C_{\text{wet}} - C_{\text{dry}})RH \quad (4)$$

where  $C_{\text{dry}}$  is the heat capacity of dry air,  $C_{\text{wet}}$  – the heat capacity of air saturated with water vapor, and  $RH$  – the relative humidity calculated:

$$RH = \min\left(\frac{m_3 R T_3}{M_{\text{H}_2\text{O}} P_a(T_3) V_3}, 1\right) \quad (5)$$

where  $R$  is the gas constant,  $M_{\text{H}_2\text{O}}$  – the molar mass of water, and  $p_a = p_a(T)$  – the saturation vapor pressure of water as a function of the temperature  $T$  given by the Tetens equation:

$$p_a = p_a(T) = 610.78 \cdot 10^{7.5(T-273.15)/(T-273.15+237.30)} \quad (6)$$

Each flux appearing in (1) or (2) is evaluated as follows.

The  $Q_{01}$  is the discharge of saline water artificially introduced from the rainwater harvesting system, which is treated as a given variable  $Q_{\text{in}}$ . The  $Q_{12}$  is the leakage of saline water

from the reservoir to the ground. Because of the plastic sheet covering the bottom of reservoir,  $Q_{12}$  is assumed to be zero. Evaporation and dew condensation play fundamental roles in the desalination plant. The evaporation  $Q_{13}$  from the reservoir surface is evaluated:

$$Q_{13} = k_{sw} D \frac{M_{H_2O}}{RT_3} \frac{p_a(T_1) - p_3}{\delta} A_1 \quad (7)$$

where  $k_{sw}$  is an evaporation coefficient to represent the effect of water salinity,  $D$  – the diffusion coefficient,  $p_3$  – the vapor pressure in the GH air,  $\delta$  – the diffusion layer thickness, and  $A_1$  ( $= 220 \text{ m}^2$ ) – the water surface area of GH reservoir. The diffusion coefficient  $D$  is represented:

$$D = 3.1475 \cdot 10^{-6} \frac{T_3^{1.9526}}{p} \quad (8)$$

which is derived from Cussler [27]. In analogy with  $Q_{13}$ ,  $Q_{35}$  – the dew condensation which can be calculated:

$$Q_{35} = D \frac{M_{H_2O}}{RT_3} \frac{p_3 - p_a(T_5)}{\delta} A_5 \quad (9)$$

where  $A_5$  is the area of GH cover,  $-Q_{45}$  – is the actual rate of dew collection by  $M_4$  (WRC), which is assumed to be proportional to the dew condensed along the GH cover:

$$Q_{45} = -k_{dc} V_5 \quad (10)$$

where  $k_{dc}$  is a dew collection coefficient. The amount of collected dew that has accumulated within the last 24 hours is denoted by  $v$ . While, another part of the condensed dew returns to  $M_1$  (GH reservoir) at a rate of  $-Q_{15}$ , which is also assumed:

$$Q_{15} = -k_{dr} V_5 \quad (11)$$

where  $k_{dr}$  is a dew returning coefficient.

The water fluxes  $Q_{01}$ ,  $Q_{15}$ , and  $Q_{45}$  accompany the heat fluxes  $C_0 T_{in} Q_{01}$ ,  $C_{wat} T_5 Q_{15}$ , and  $C_{wat} T_5 Q_{45}$ , respectively. Latent heat is considered within the processes of evaporation and dew condensation as  $HQ_{13}$  and  $HQ_{35}$ , respectively, where  $H$  is the heat of evaporation. The solar radiation  $R_{sol}$  – the exclusive source of energy in the desalination plant, absorbed by each medium  $M_i$  with an absorption coefficient  $\alpha_i$ . Firstly,  $M_5$  (GH cover) absorbs a portion  $\alpha_5 R_{sol} A_0$  of the total solar radiation  $R_{sol} A_0$ , and another portion  $k_{tr} R_{sol} A_0$  transmits  $M_5$ , where  $k_{tr}$  is the transmittance of GH cover. Then, the solar radiation transmitted through  $M_5$  is absorbed by the other four media inside GH. While, the long wave radiation between different two medium occurs according to the Stefan-Boltzmann law. The Stefan-Boltzmann constant is denoted by  $\sigma$ . When the medium  $M_0$  (ambient) or the medium  $M_3$  (GH air) is not involved, an effective area  $A_{ij}^E$  from the medium  $M_i$  to the medium  $M_j$  is evaluated:

$$\frac{1}{A_{ij}^E} = \frac{1 - \varepsilon_i}{\varepsilon_i A_i} + \frac{1}{F_{ij}^V A_i} + \frac{1 - \varepsilon_j}{\varepsilon_j A_j} \quad (12)$$

where  $\varepsilon_i$  is the emissivity of the medium  $M_i$ , and  $F_{ij}^V$  – the view factor from the medium  $M_i$  to the medium  $M_j$ . The medium  $M_3$  (GH air) absorbs a part of the radiation entering from the other medium due to the GH effect. When a media is in contact with the air mass, heat transfer is assumed to take place in proportion the thermal difference with a heat transfer coefficient  $\kappa_{air}$  of air. Finally, the heat flux between each pair of the 15 combinations of the media is estimated:

$$P_{01} = C_{in} T_{in} Q_{01} + \alpha_1 k_{tr} R_{sol} A_1 \quad (13)$$

$$P_{02} = \alpha_2 k_{tr} R_{sol} A_2 \quad (14)$$

$$P_{03} = \alpha_3 k_{tr} R_{sol} A_0 \quad (15)$$

$$P_{04} = \alpha_4 k_{tr} R_{sol} A_4 \quad (16)$$

$$P_{05} = \alpha_5 R_{sol} A_0 + \sigma \varepsilon_5 T_5^4 A_5 + \kappa_{air} (T_0 - T_5) A_5 \quad (17)$$

$$P_{12} = 0 \quad (18)$$

$$P_{13} = HQ_{13} + \alpha_3 \sigma \varepsilon_1 T_1^4 A_1 + \kappa_{air} (T_1 - T_3) A_1 \quad (19)$$

$$P_{14} = \sigma (T_1^4 - T_4^4) A_{14}^E \quad (20)$$

$$P_{15} = \sigma (T_1^4 - T_5^4) A_{15}^E \quad (21)$$

$$P_{23} = \alpha_3 \sigma \varepsilon_2 T_2 A_2 + \kappa_{air} (T_2 - T_3) A_2 \quad (22)$$

$$P_{24} = \sigma (T_2^4 - T_4^4) A_{24}^E \quad (23)$$

$$P_{25} = \sigma (T_2^4 - T_5^4) A_{25}^E \quad (24)$$

$$P_{34} = -\alpha_3 \sigma \varepsilon_4 T_4^4 A_4 + \kappa_{air} (T_3 - T_4) A_4 \quad (25)$$

$$P_{35} = HQ_{35} - \alpha_3 \sigma \varepsilon_5 T_5^4 A_5 + \kappa_{air} (T_3 - T_5) A_5 \quad (26)$$

$$P_{45} = C_w T_5 Q_{45} + \sigma (T_4^4 - T_5^4) A_{45}^E \quad (27)$$

The aforementioned eqs. (1)-(27) constitute a closed ODE system. Initial value problems of the ODE system with different values of the model parameters are numerically solved to calibrate them.

#### Measurement of physical parameters

Different physical parameters are being measured inside GH as well as in the ambient. Among those parameters, the items summarized in tab. 1 are used for examining the concept of the model. The manual dew collection using a bucket is performed daily except on holidays, taking about 10 minutes. Therefore, the interval is not fixed at exactly 24 hours. The amount of dew collected each day is recorded with an accuracy of 1 L, as read 3 digits after the decimal point are doubtful. The other physical parameters measured with the digital devices have 4 digits accuracy at least. A complete set of measured data is available for the 371 days period from February 23, 2017 through February 28, 2018. Saline water was introduced to GH reservoir on February 23, 2017 and February 24, 2017, and thereafter no water was added to GH reservoir.

**Table 1. Measured physical parameters to be used in the model**

Measurement item	Device	Interval	Usage in the model
Solar radiation, $R_{sol}$ [ $\text{Wm}^{-2}$ ]	Hukseflux SR05	30 minute	Input
Ambient air temperature, $T_0$ [K]	VAISALA WXT520	10 minute	Input
GH reservoir water temperature, $T_1$ [K]	HOBO TidbiT	10 minute	Calibration
GH air temperature, $T_3$ [K]	HOBO U23 Pro v2	10 minute	Calibration
GH relative humidity, $RH$ [-]	HOBO U23 Pro v2	10 minute	Reference
Amount of collected dew, $v$ [L]	Manual using a bucket	1 day	Reference

## Results and discussion

### *Known and calibrated model parameters*

Table 2 summarizes the model parameters whose values are widely accepted. While, tab. 3 presents the values of model parameter values calibrated to achieve an acceptable level of accordance with the measured time series as indicated in tab. 1. Both sides are considered for heat absorption of WRC, which is hanged inside GH. The emissivity  $\varepsilon_5$  of GH cover is eventually one of the most sensitive parameters. The diffusion layer sickness  $\delta$  and the heat transfer coefficient  $\kappa_{\text{air}}$  of air are two thermal fluid mechanical paramters taking relatively small values inside GH where convection is not dominant.

**Table 2. Known values of model parameters**

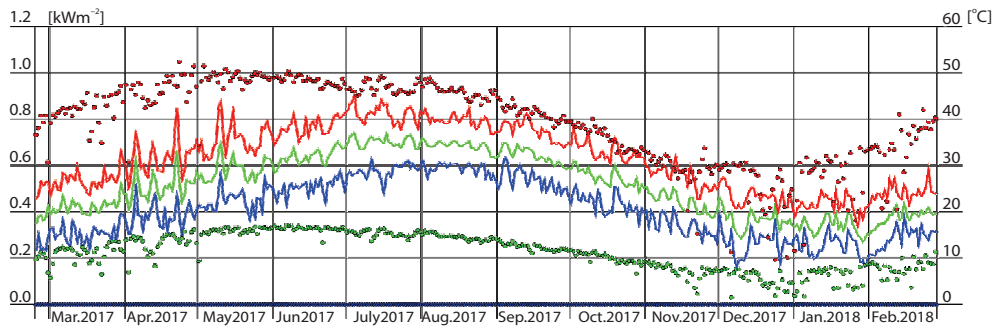
Model parameter	Symbol	Value	Unit
Heat capacity of dry air	$C_{\text{dry}}$	$1.005 \cdot 10^3$	$[\text{Jkg}^{-1}\text{K}^{-1}]$
Heat capacity of air saturated with water vapor	$C_{\text{wet}}$	$1.030 \cdot 10^3$	$[\text{Jkg}^{-1}\text{K}^{-1}]$
Heat capacity of freshwater	$C_{\text{wat}}$	$4.180 \cdot 10^3$	$[\text{Jkg}^{-1}\text{K}^{-1}]$
Heat capacity of ground (PVC sheets)	$C_2$	$1.300 \cdot 10^3$	$[\text{Jkg}^{-1}\text{K}^{-1}]$
Heat capacity of WRC	$C_4$	$1.300 \cdot 10^3$	$[\text{Jkg}^{-1}\text{K}^{-1}]$
Heat capacity of GH cover (PE sheets)	$C_5$	$9.000 \cdot 10^2$	$[\text{Jkg}^{-1}\text{K}^{-1}]$
Molar mass of water	$M_{\text{H}_2\text{O}}$	$1.802 \cdot 10^{-2}$	$[\text{kgmol}^{-1}]$
Gas constant	R	$8.314 \cdot 10^{-3}$	$[\text{JK}^{-1}\text{mol}^{-1}]$
Heat of evaporation	$H$	$2.257 \cdot 10^6$	$[\text{Jkg}^{-1}]$
Stefan-Boltzmann constant	$\sigma$	$5.670 \cdot 10^{-8}$	$[\text{Wm}^{-2}\text{K}^{-4}]$

**Table 3. Calibrated values of model parameters**

Model parameter	Symbol	Value	Unit
Evaporation coefficient	$k_{\text{sv}}$	0.90	$[-]$
Diffusion layer thickness	$\delta$	0.10	$[\text{m}]$
Dew collection coefficient	$k_{\text{dc}}$	$2.0 \cdot 10^{-3}$	$[\text{s}^{-1}]$
Dew returning coefficient	$k_{\text{dr}}$	$1.0 \cdot 10^{-3}$	$[\text{s}^{-1}]$
Heat transfer coefficient of air	$\kappa_{\text{air}}$	20	$[\text{Wm}^{-2}\text{K}^{-1}]$
Transmittance of GH cover	$k_{\text{tr}}$	0.85	$[-]$
Absorption coefficient of GH reservoir water	$\alpha_1$	0.50	$[-]$
Absorption coefficient of GH ground	$\alpha_2$	0.97	$[-]$
Absorption coefficient of GH air	$\alpha_3$	0.20 RH	$[-]$
Absorption coefficient of WRC	$\alpha_4$	$0.97 \cdot 2$	$[-]$
Absorption coefficient of GH cover	$\alpha_5$	0.05	$[-]$
Emissivity of GH reservoir water	$\varepsilon_1$	0.95	$[-]$
Emissivity of GH ground	$\varepsilon_2$	0.95	$[-]$
Emissivity of WRC	$\varepsilon_4$	0.95	$[-]$
Emissivity of GH cover	$\varepsilon_5$	0.50	$[-]$
Vision factor from GH reservoir to WRC	$F_{14}^V$	0.05	$[-]$
Vision factor from GH reservoir to GH cover	$F_{15}^V$	0.95	$[-]$
Vision factor from GH ground to WRC	$F_{24}^V$	0.95	$[-]$
Vision factor from GH ground to GH cover	$F_{25}^V$	0.05	$[-]$
Vision factor from WRC to GH cover	$F_{45}^V$	0.80	$[-]$

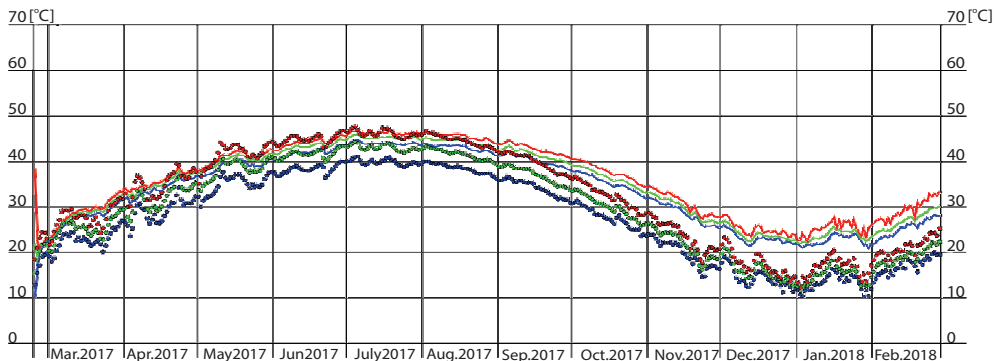
### Measured and simulated physical parameters

Figure 2 outlines the input data, which are the solar radiation  $R_{\text{sol}}$  and the ambient air temperature  $T_0$ , in terms of daily average, minimum, and maximum during the whole study period of 371 days. Different time lags can be seen in the peaks and bottoms of daily average, minimum, and maximum temperature from those of solar radiation. Weather in general is unstable during the winter season from November through April.



**Figure 2.** Measured daily average (green), minimum (blue), and maximum (red) solar radiation (dots) and ambient air temperature (lines) (for color image see journal web site)

Results of measurement and simulation are compared in figs. 3 and 4 for the temperature  $T_1$  of GH reservoir and the temperature  $T_3$  of GH air, respectively. Numerical reproduction of the full thermal dynamics is a significant advantage of the developed model over the steady-state model of Chaibi [8]. Calibration has been done so that the simulated daily maximums of  $T_1$  and  $T_3$  reasonably follow the measured ones during early stages of the study period, and discrepancy between measurement and simulation as a whole is not negligible. Heat capacity of the water in GH reservoir may be higher in the reality than in the model, as the slower response of measured  $T_1$  in fig. 3 suggests. Fluctuations in  $T_3$  are reasonably simulated as in fig. 4, where the discrepancy is of bias error. Nevertheless, simulated amount  $v$  of collected dew is comparable with the actual amount, as plotted in fig. 5. Leveling-off of actual dew collection during the months of May through October is due to the limited sizes of the apparatus used. Indeed, the PET bottles have been replaced with containers of a larger size since August 2018, resulting in drastic increase in actual dew collection support the simulation results. However, automatization of dew collection process is still recommended to improve efficiency of the desalination plant.



**Figure 3.** Measured (lines) and simulated (dots) daily average (green), minimum (blue), and maximum (red) temperature of GH reservoir (for color image see journal web site)

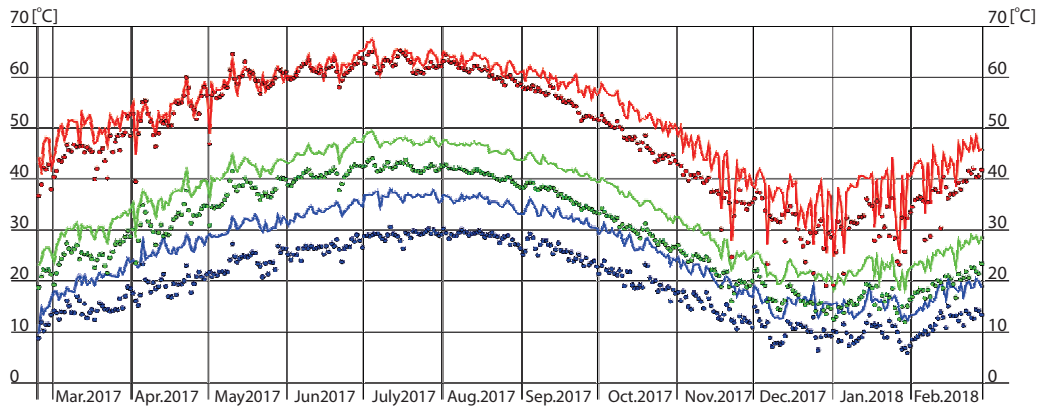


**Figure 4.** Measured (lines) and simulated (dots) daily average (green), minimum (blue), and maximum (red) temperature of GH air (for color image see journal web site)

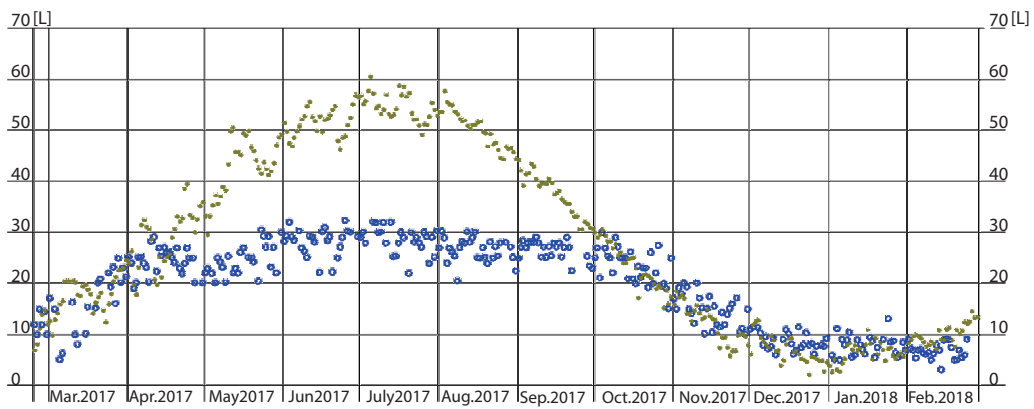


**Figure 5.** Actual (circles) and simulated (dots) amounts of collected dew

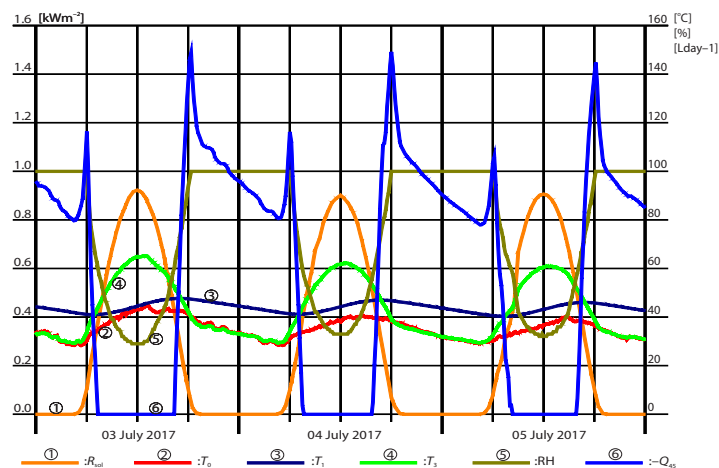


**Figure 6.** Simulated dynamics of physical parameters for three days where high yield of dew was reproduced

### Dynamics of the model

Simulated dynamics of the physical parameters are presented in figs. 6 and 7 for the three days periods of July 03-05, 2017 (summer) and December 23-25, 2017 (winter), respectively. The periods have been chosen because the highest and the lowest yields of dew,  $-Q_{45}$ , are predicted on July 04, 2017 and December 24, 2017, respectively. In the hottest hours of day time, there is no yield of dew. For the summer period,  $-Q_{45}$ , sharply increases in evening hours and then gradually decreases after sunset, before another sharp peak immediately after sunrise. However, unstable weather condition during the winter period results in uncertain yield of dew.

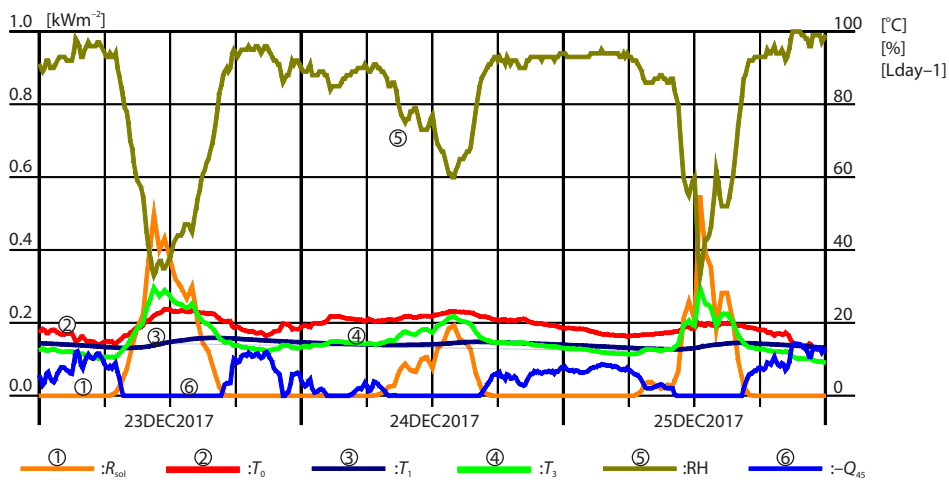


Figure 7. Simulated dynamics of physical parameters for three days where low yield of dew was reproduced

### Conclusion

The prototype of solar driven desalination plant is successfully operating in LP to produce fresh water for irrigation. The measurement and simulation results show that the model, which is mathematically stable, well explains the complex thermal dynamical mechanisms of the plant yielding dew, which is manually collected. The dew yield is sensitive to the meteorological inputs, mostly synchronized with the ambient air temperature. The substantial potential yield of dew was not collected during the summer period of the year 2017, however, the dew collection process has been drastically improved since August 2018. The concept of this solar driven desalination plant can be disseminated to other arid environments having very hot stable dry seasons.

### Acknowledgment

This research is funded by Invitation Fellowship for Research in Japan No. L145461 and Grants-in-Aid for Scientific Research No. 26257415 and No. 16KT0018, from the Japan Society for the Promotion of Science (JSPS). This work was done partially during Dr. Osama Mohawesh sabbatical leave from Mutah Universtiy in Kyoto University.

### Nomenclature

$A_1$  – water surface area of GH reservoir, [m<sup>2</sup>]  
 $A_5$  – area of GH cover, [m<sup>2</sup>]

$A_{ij}^E$  – effective area from the medium  $M_i$  to the medium  $M_j$ , [m<sup>2</sup>]  
 $C_i$  – heat capacity of the medium  $M_i$ , [Jkg<sup>-1</sup>K<sup>-1</sup>]

$C_{\text{dry}}$ – heat capacity of dry air, [ $\text{Jkg}^{-1}\text{K}^{-1}$ ]	$R_{\text{sol}}$ – solar radiation, [ $\text{Wm}^{-2}$ ]
$C_{\text{wat}}$ – heat capacity of freshwater, [ $\text{Jkg}^{-1}\text{K}^{-1}$ ]	$RH$ – relative humidity, [–]
$C_{\text{wet}}$ – heat capacity of air saturated with water vapor, [ $\text{Jkg}^{-1}\text{K}^{-1}$ ]	$T_i$ – temperature of the medium $M_i$ , [K]
$c$ – concentration of salt, [–]	$t$ – time, [s]
$D$ – diffusion coefficient, [ $\text{m}^2\text{s}^{-1}$ ]	$V_i$ – volume of water stored in the medium $M_i$ , [ $\text{m}^3$ ]
$F_{ij}^V$ – view factor from the medium $M_i$ to the medium $M_j$ , [–]	$v$ – amount of collected dew that has accumulated within the last 24 hours, [ $\text{m}^3$ ]
$H$ – heat of evaporation, [ $\text{Jkg}^{-1}$ ]	
$k_{\text{dc}}$ – dew collection coefficient, [ $\text{s}^{-1}$ ]	<b>Greek symbols</b>
$k_{\text{dr}}$ – dew returning coefficient, [ $\text{s}^{-1}$ ]	$\alpha_i$ – absorption coefficient of the medium $M_i$ , [–]
$k_{\text{sv}}$ – evaporation coefficient, [–]	$\delta$ – diffusion layer thickness, [m]
$k_{\text{tr}}$ – transmittance of GH cover, [–]	$\varepsilon_i$ – emissivity of the medium $M_i$ , [–]
$M_i$ – the $i^{\text{th}}$ medium	$\kappa_{\text{air}}$ – heat transfer coefficient of air, [ $\text{Wm}^{-2}\text{K}^{-1}$ ]
$M_{\text{H}_2\text{O}}$ – molar mass of water, [ $\text{kgmol}^{-1}$ ]	$\sigma$ – Stefan-Boltzmann constant, [ $\text{Wm}^{-2}\text{K}^{-4}$ ]
$m_i$ – mass of the medium $M_i$ , [kg]	
$P_{ij}$ – heat flux flowing from the medium $M_i$ to the medium $M_j$ , [W]	<b>Acronyms</b>
$p_a$ – saturation vapor pressure of water, [Pa]	GH – greenhouse
$p_3$ – vapor pressure in the GH air, [Pa]	LP – Lisan Peninsula
$Q_{ij}$ – water mass flux flowing from the medium $M_i$ to the medium $M_j$ , [ $\text{m}^3\text{s}^{-1}$ ]	PE – polyethylene
$R$ – gas constant, [ $\text{JK}^{-1}\text{mol}^{-1}$ ]	PVC – polyvinyl chloride
	WRC – water repellent cloth

## References

- [1] Salameh, E., Sources of Water Salinities in the Jordan Valley Area/Jordan, *Acta Hydrochimica et Hydrobiologica*, 29 (2001), 6-7, pp. 329-362
- [2] Mohawesh, O., Utilizing Deficit Irrigation Enhance Growth Performance and Water use Efficiency of Eggplant in Arid Environments, *Journal of Agricultural Science and Technology*, 18 (2016), 1, pp. 265-276
- [3] Unami, K., *et al.*, Stochastic Modelling and Control of Rainwater Harvesting Systems for Irrigation during Dry Spells, *Journal of Cleaner Production*, 88 (2015), Feb., pp. 185-195
- [4] Unami, K., Mohawesh, O., A Unique Value Function for an Optimal Control Problem of Irrigation Water Intake from a Reservoir Harvesting Flash Floods, *Stochastic Environmental Research and Risk Assessment*, 32 (2018), Mar., pp. 3169-3182
- [5] Perret, J. S., *et al.*, Development of a Humidification-Dehumidification System in a Quonset Greenhouse for Sustainable Crop Production in Arid Regions, *Biosystems Engineering*, 91 (2005), 3, pp. 349-359
- [6] Jolliet, O., HORTITRANS, A Model for Predicting and Optimizing Humidity and Transpiration in Greenhouses, *Journal of Agricultural Engineering Research*, 57 (1994), 1, pp. 23-37
- [7] Goosen, M. F. A., *et al.*, Capacity Building Strategies for Desalination: Activities, Facilities and Educational Programs in Oman, *Desalination*, 141 (2001), 2, pp. 181-190
- [8] Chaibi, M. T., Analysis by Simulation of a Solar Still Integrated in a Greenhouse Roof, *Desalination*, 128 (2000), 2, pp. 123-138
- [9] Hao, X.-M., *et al.*, Dew Formation and Its Long Term Trend in a Desert Riparian Forest Ecosystem on the Eastern Edge of the Taklimakan Desert in China, *Journal of Hydrology*, 472-473 (2012), pp. 90-98
- [10] Greenlee, L. F., *et al.*, Reverse Osmosis Desalination: Water Sources, Technology, and Today's Challenges, *Water Research*, 43 (2009), 9, pp. 2317-2348
- [11] Malik, M. A. S., *et al.*, *Solar Distillation: A Practical Study of a Wide Range of Stills and Their Optimum Design, Construction and Performance*, Pergamon Press Ltd., Oxford, UK, 1996
- [12] Chaibi, M. T., Validation of a Simulation Model for Water Desalination in a Greenhouse Roof through Laboratory Experiments and Conceptual Parameter Discussions, *Desalination*, 142 (2002), 1, pp. 65-78
- [13] Medina, J. A., Feasibility of Water Desalination for Agriculture-from Water Desalination for Agricultural Applications, in: *Land and Water Discussion Paper* (Ed. Beltran, J. M., Oshima, S. K.), FAO, Rome, 2006, pp. 37-44
- [14] Zhani, K. Solar Desalination Based on Multiple Effect Humidification Process: Thermal Performance and Experimental Validation, *Renewable and Sustainable Energy Reviews*, 24 (2013), C, pp. 406-417

- [15] Mashaly, A., *et al.*, Area Determination of Solar Desalination System for Irrigating Crops in Greenhouses Using Different Quality Feed Water, *Agricultural Water Management*, 154 (2015), May, pp. 1-10
- [16] Oroud, I., The Impacts of Climate Change on Water Resources in Jordan, in: *Climatic Changes and Water Resources in the Middle East and North Africa* (Ed. Zereini, F., Hotzl, H.), Springer-Verlag, Berlin Heidelberg, 2008, 4, pp. 109-123
- [17] Matouq, M., *et al.*, The Climate Change Implication on Jordan: A Case Study Using GIS and Artificial Neural Networks for weather forecasting, *Journal of Taibah University for Science*, 7 (2013), 2, pp. 44-55
- [18] Mohawesh, O., Development of Pedotransfer Functions for Estimating Soil Retention Curves and Saturated Hydraulic Conductivity in Jordan Valley, *Jordan Journal of Agricultural Sciences*, 10 (2014), 1, pp. 67-82
- [19] Molle, F., *et al.*, Irrigation in the Jordan Valley: Are Water Pricing Policies Overly Optimistic, *Agricultural Water Management*, 95 (2008), 4, pp. 427-438
- [20] Amayreh, J., Al-Abed, N., Developing Crop Coefficients for Field-Grown Tomato (*Lycopersicon Esculentum* Mill.) under Drip Irrigation with Black Plastic Mulch, *Agricultural Water Management*, 73 (2005), 3, pp. 247-254
- [21] Mahadeen, A. Y., *et al.*, Effect of Irrigation Regimes on Water use Efficiency and Tomato Yield (*Lycopersicon Esculentum* Mill.) Grown in an Arid Environment, *Archives of Agronomy and Soil Science*, 57 (2011), 1, pp. 105-114
- [22] \*\*\*, Jordan Valley Authority, General Information, *Proceedings*, 3<sup>rd</sup> Country Training Programme for Water Resources Management, Ministry of Water and Irrigation, The Hashemite Kingdom of Jordan, Amman, Jordan, 2004
- [23] Harmanto, V. M., *et al.*, Water Requirement of Drip Irrigated Tomatoes Grown in Greenhouse in Tropical Environment, *Agricultural Water Management*, 71 (2005), 3, pp. 225-242
- [24] Ammari, T. G., *et al.*, Soil Salinity Changes in the Jordan Valley Potentially Threaten Sustainable Irrigated Agriculture, *Pedosphere*, 23 (2013), 3, pp. 376-384
- [25] Sharifi, E., *et al.*, Design and Construction of a Hydraulic Structure for Rainwater Harvesting in Arid Environment, *E-Proceedings*, 36<sup>th</sup> IAHR World Congress, Hague, The Netherlands, 2015, pp. 3375-3386
- [26] Sun, H., *et al.*, New Equations for Density, Entropy, Heat Capacity, and Potential Temperature of a Saline Thermal Fluid, *Deep-Sea Research I*, 55 (2008), 10, pp.1304-1310
- [27] Cussler, E. L., *Diffusion: Mass Transfer in Fluid Systems*, 3<sup>th</sup> ed., Cambridge University Press, New York, USA, 2009